iScience, Volume *23*

Supplemental Information

Generation of a Single-Cell RNAseq

Atlas of Murine Salivary Gland Development

Belinda R. Hauser, Marit H. Aure, Michael C. Kelly, Genomics and Computational Biology Core, Matthew P. Hoffman, and Alejandro M. Chibly

Supplementary Figure S1, related to figure 1

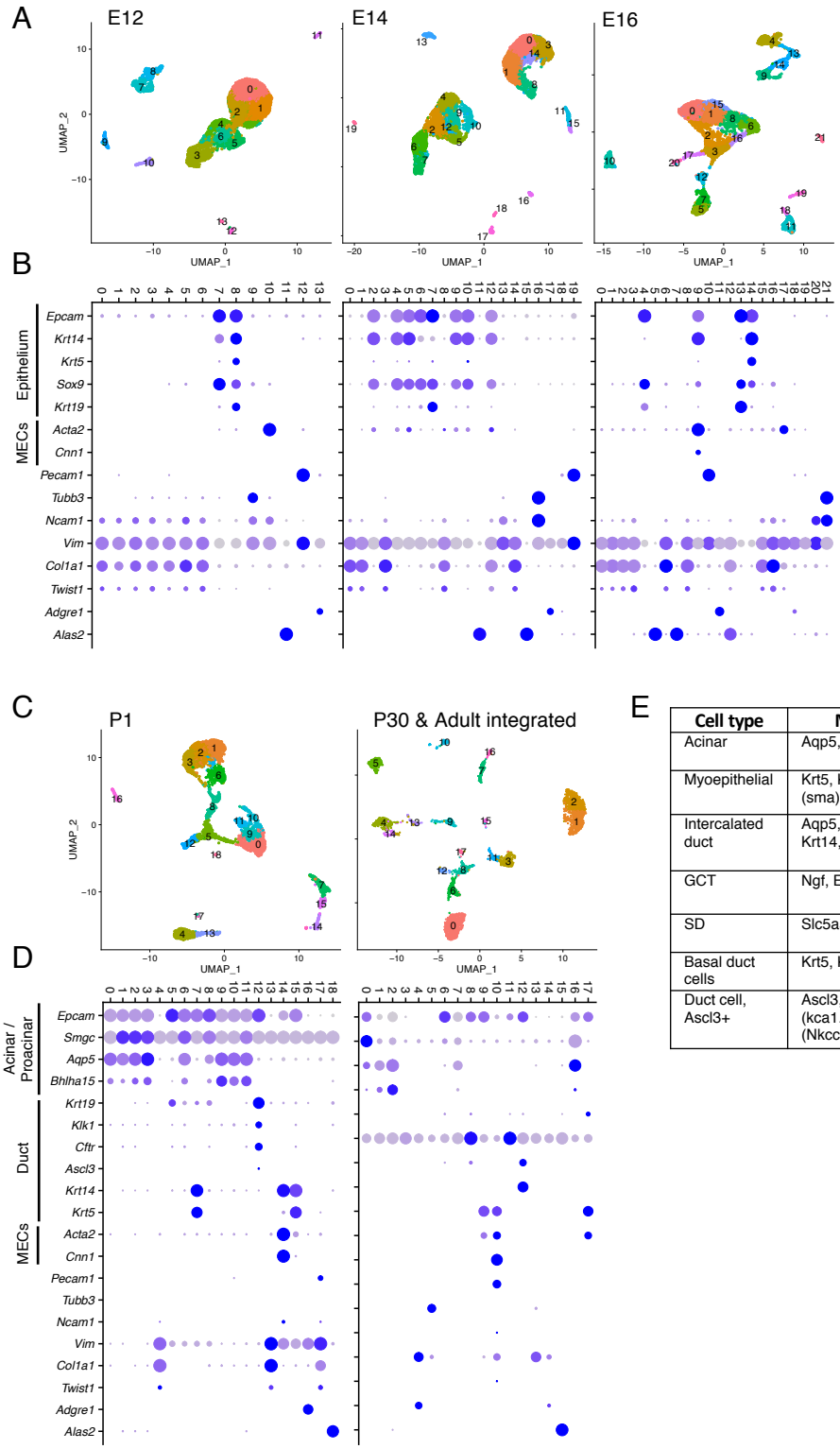

E

Cell type	Marker	Reference
Acinar	Aqp5, Bhlha15	(Larsen et al., 2011, Johnson et al., 2004)
Myoepithelial	Krt5, Krt14, Acta2 (sma), Cnn1	(Nelson et al., 2013)
Intercalated duct	Aqp5, Smgc, Krt14, c-kit	(Kwak et al., 2016, Larsen et al., 2011, Kusakabe et al., 2016)
GCT	Ngf, Egf	(Gresik, 1994, Hazen-Martin et al., 1987)
SD	Slc5a5, Cftr	(Zeng et al., 2017, Dohan et al., 2003)
Basal duct cells	Krt5, Krt14, trp63	(Nelson et al., 2013)
Duct cell, Ascl3+	Ascl3, Kcnma1 (kca1.1), Slc12a2 (Nkcc1)	(Arany et al., 2011)

Supplementary Figure 2. Annotation strategy.

Cell clustering was performed for individual developmental stages to annotate cell populations based on known cell markers prior to data integration.
A) UMAPs showing unsupervised clustering of scRNAseq from embryonic SMG.
B) Dot plot showing expression of markers used for annotation of embryonic SMG (MECs = myoepithelial cells).
C) UMAPs showing unsupervised clustering of scRNAseq from postnatal SMG.
D) Dot plot showing expression of markers used for annotation of postnatal SMG
E) Table with references to known epithelial markers for specific cell types in adult salivary glands.
Non-epithelial markers: *Pecam1*: Endothelial; *Tubb3*: Nerves; *Ncam1*: Nerves and Glial cells; *Vim, Col1a1 & Twist1*: Mesenchymal and stromal cells; *Adgre1*: Macrophages; *Alas2*:Erythroid; *Acta2*: Myoepithelial and smooth muscle cells.

Supplementary Figure S2, related to figure 2

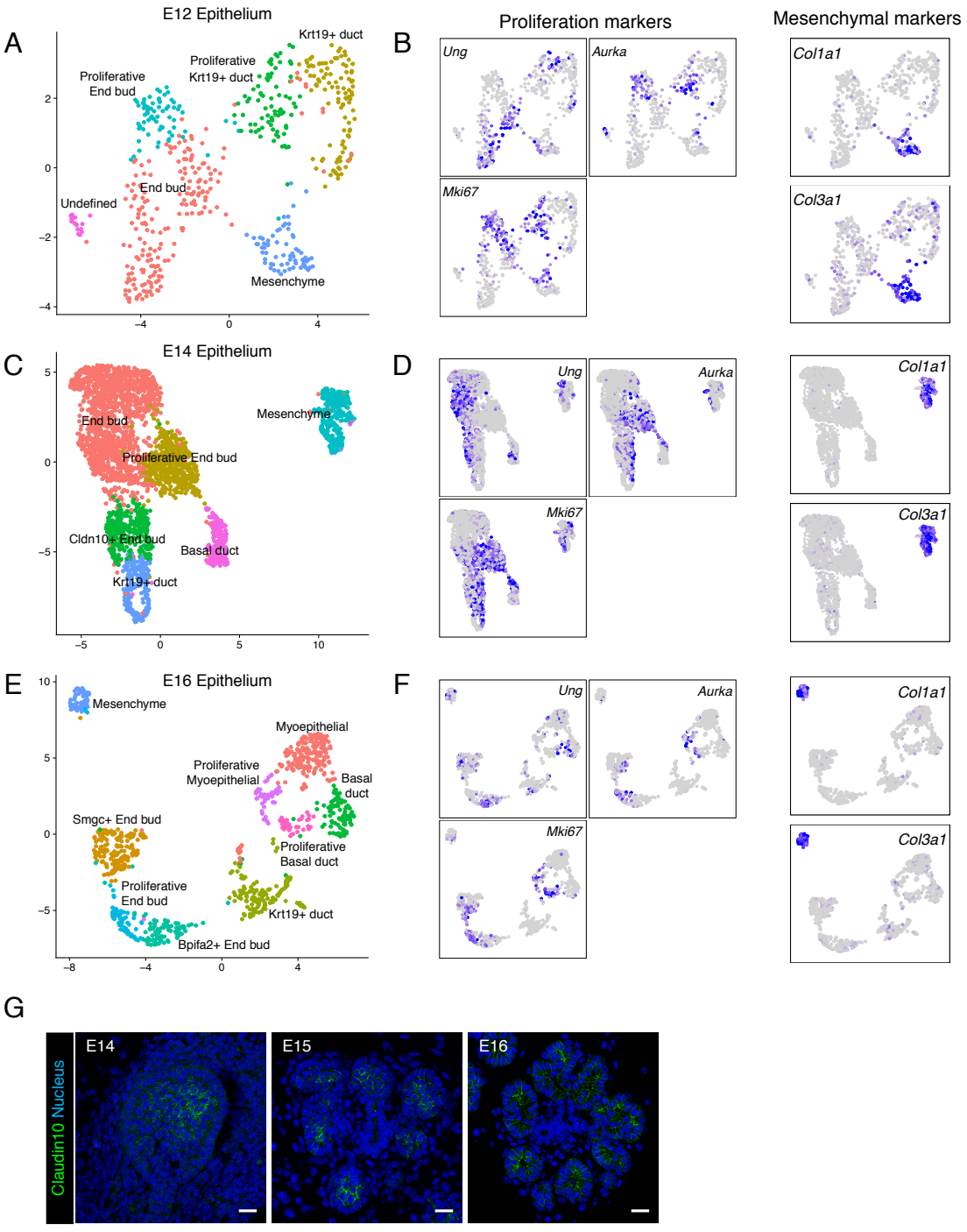

Supplementary Figure 3: Proliferative epithelial subpopulations in embryonic SMG

A) Annotated subpopulations in E12 SMG epithelium.
B) UMAP showing subpopulations of proliferative and mesenchymal markers in E12 SMG epithelial cells.
C) Annotated subpopulations in E14 SMG epithelium.
D) UMAP showing subpopulations of proliferative and mesenchymal markers in E14 SMG epithelial cells.
E) Annotated subpopulations in E16 SMG epithelium.
F) UMAP showing subpopulations of proliferative and mesenchymal markers in E16 SMG epithelial cells.
G) Immunostaining for claudin 10 (green) in embryonic SMG

Supplementary Figure S3, related to figure 3

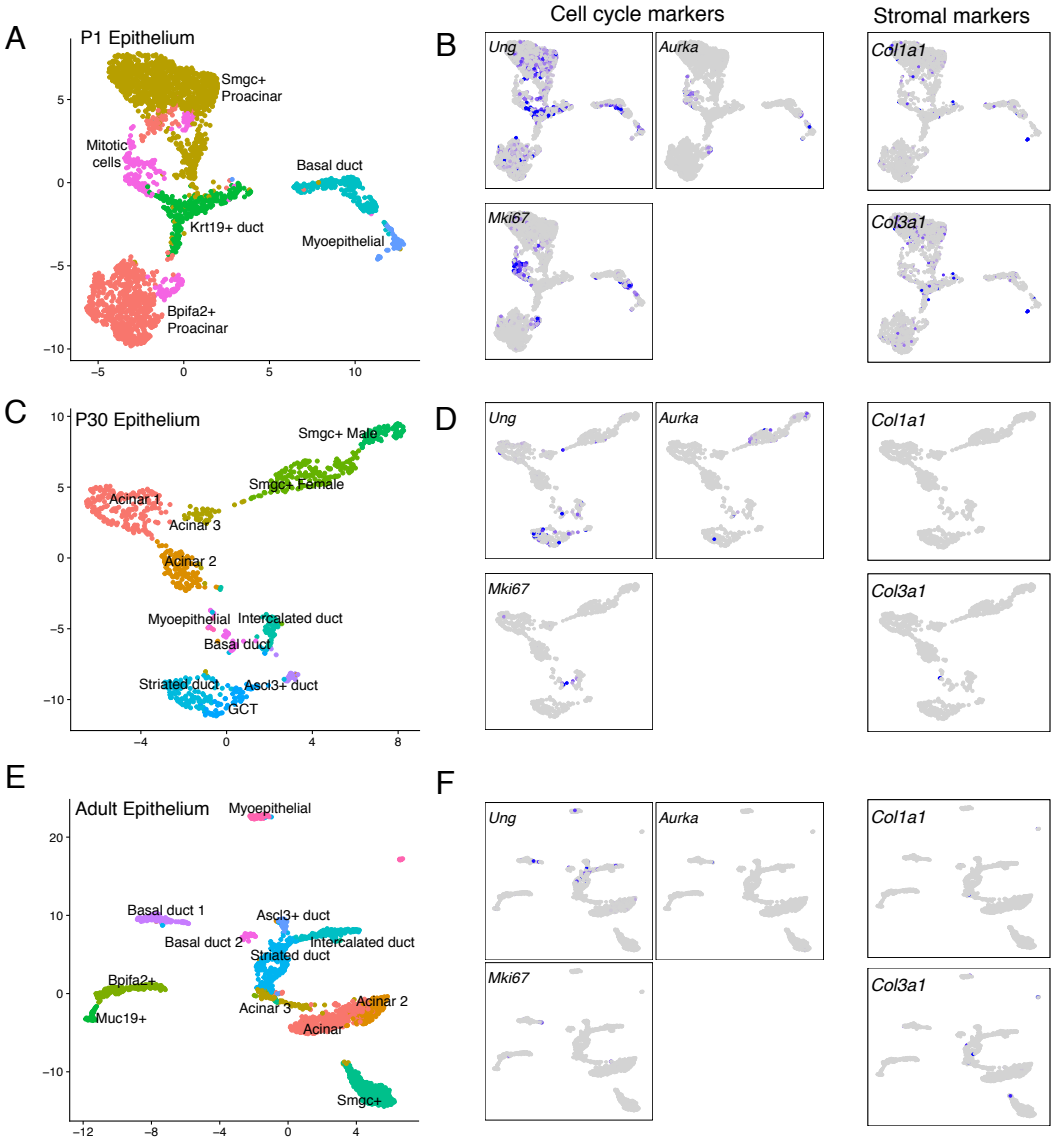

Supplementary Figure 3: Proliferative epithelial subpopulations in postnatal SMG

A) Annotated subpopulations in P1 SMG epithelium.
B) UMAP showing subpopulations of proliferative and stromal markers in P1SMG epithelial cells.
C) Annotated subpopulations in P30 SMG epithelium.
D) UMAP showing subpopulations of proliferative and stromal markers in 30 SMG epithelial cells.
E) Annotated subpopulations in Adult SMG epithelium.
F) UMAP showing subpopulations of proliferative and stromal markers in Adult SMG epithelial cells.

Figure S4, Related to Figure 5

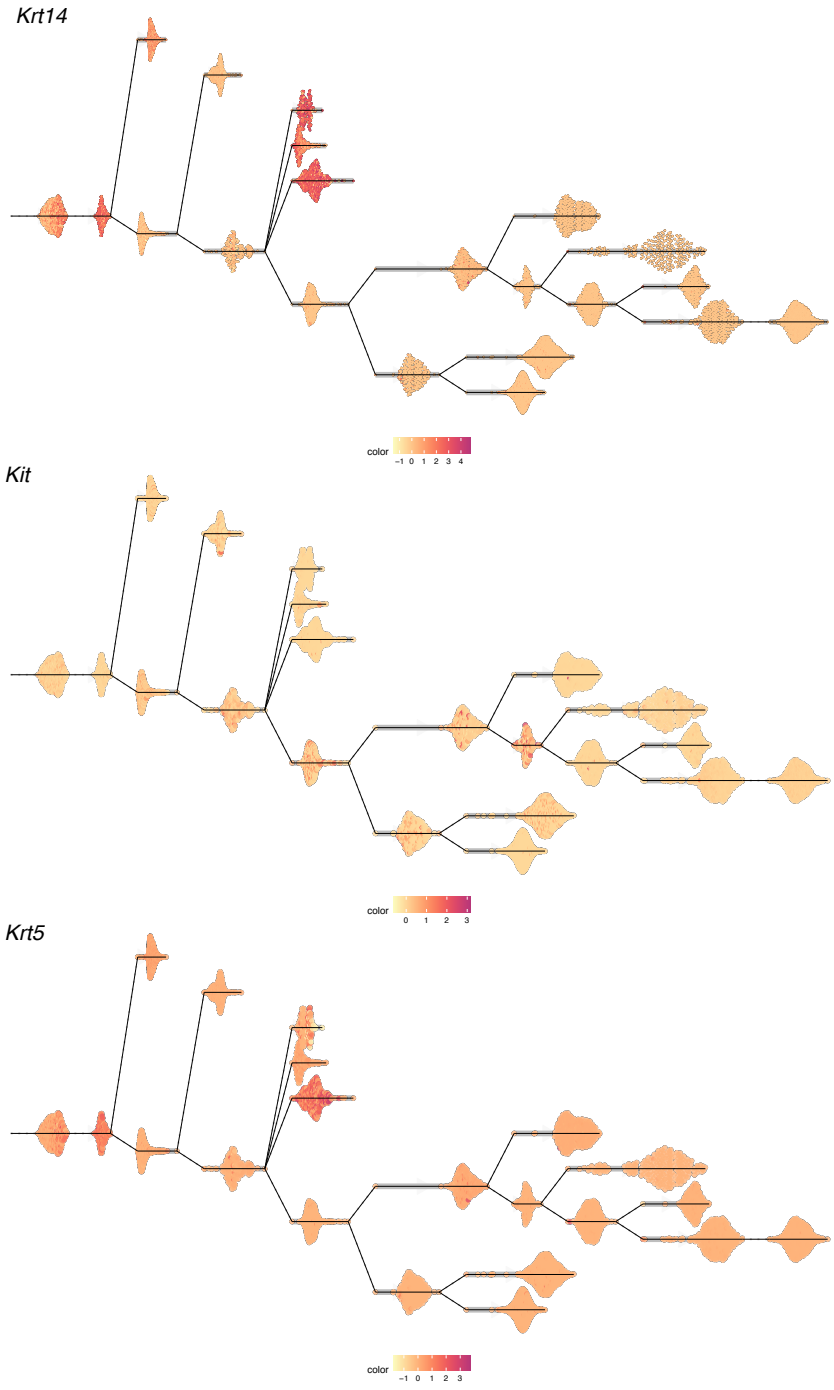

Supplementary Figure S4. Expression of Krt14, Kit, and Krt5 along pseudotime trajectory. Intensity of color is relative to the scaled gene expression across all cells in the integrated dataset

Supplementary Figure S5, related to figure 6

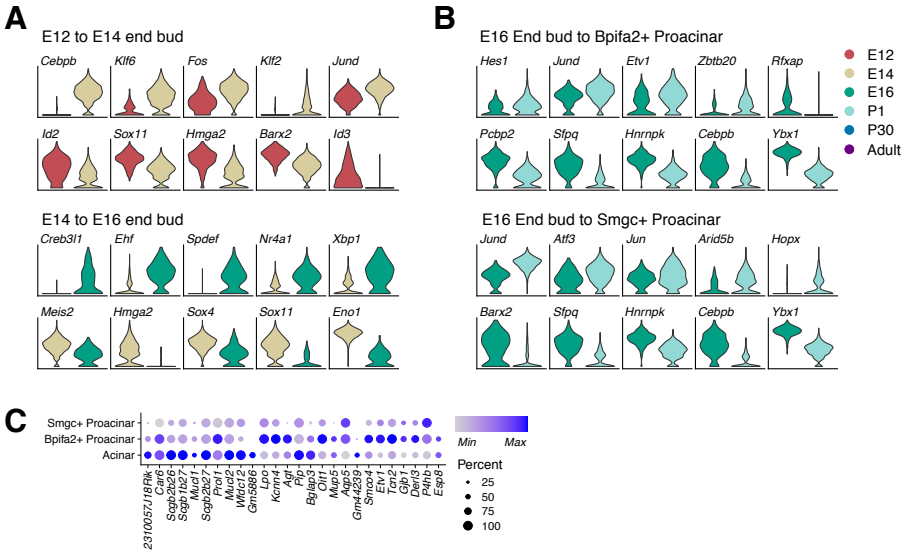

Figure S6: Differential expression analysis of end bud populations during early embryonic development

A) Top transcription factors (TFs) differentially expressed in end buds from E12 to E14 (top panel), and E14 to E16 (bottom panel).

B) Top TFs differentially expressed in the transition from end buds at E16 to proacinar cells at P1.

C) Expression levels of the 26 defining genes for seromucous acinar cells from P30 SMG across acinar and proacinar cells. Gene list is associated with the Venn Diagram in Figure 6F. The size of the dot is relative to the percentage of cells expressing a gene, and the color scale is relative to the level of expression.

Supplementary Figure S6. Related to Figure 8

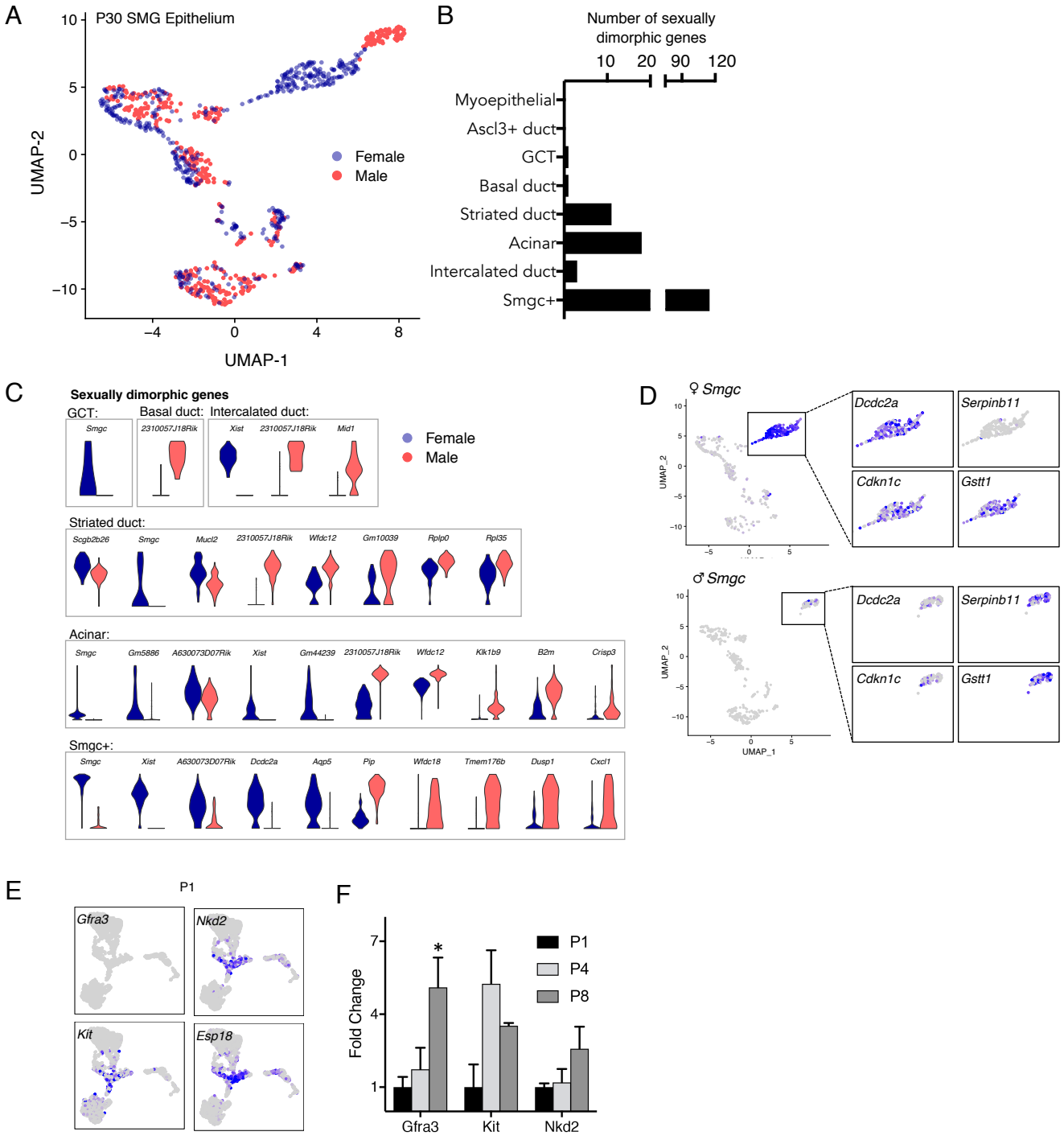

Figure S4: Sexually dimorphic genes in P30 SMG

A) UMAP of P30 SMG separated by sex.

B) Graph showing number of differentially expressed genes (DEGs) identified per cell type in female vs males.

C) Violin plots showing top 10 sexually dimorphic genes identified per cell type. All genes are shown for groups with less than 10 DEGs.

D) Representative female and male-specific genes in Smgc+ cells, as well as *Gstt1* which is common for both.

E) UMAP of expression of Gfra3+ID defining genes in P1 SMG

F) PCR results of *Gfra3, Kit,* and *Nkd2* expression in postnatal SMG normalized to P1 glands. Data are shown as the mean +/- SEM and asterisks represent statistical significance ($p<0.05$) compared to P1 SMG (n=3, two tailed t-test).

Supplementary Figure S7. Related to Figure 8

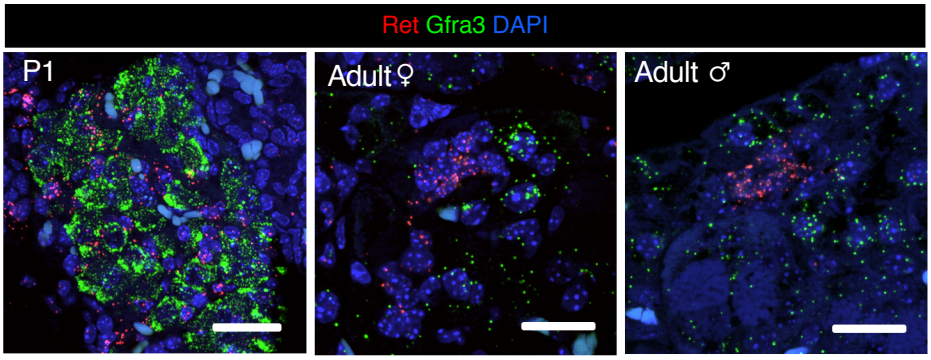

Figure S7
In situ hybridization of *Ret* (red) and *Gfra3* (green). At P1, these genes are co-expressed in ganglia. In the adult gland both male and females express *Gfra3* in ID, while *Ret* is found in acinar cells. All scale bars = 20μm.

Supplementary Figure S8, related to Figure 9

A

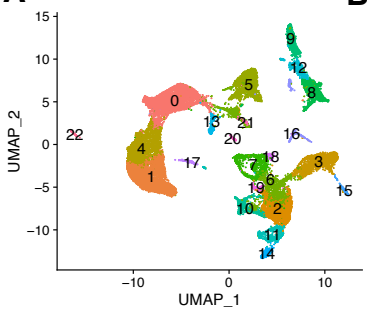

B

Cluster #	Gfra3 ID cells	Gstt1 ID cells
0	3	23
2	137	184
3	0	3
5	0	2
6	42	391
7	2	1
8	1	2
9	0	2
10	2	0
16	8	0
17	0	1

C

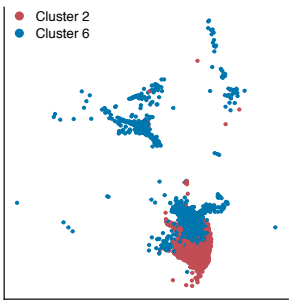

D

Original annotation from Tabula Muris	Tissue	Cluster 2 (number of cells)
LuminalB	Bladder	372
LuminalA1	Bladder	262
Basal	Bladder	256
Luminal epithelial progenitors Cd14+	Mammary	214
LuminalA2	Bladder	210
Gstt1 ID	SMG	184
Hormone responsive luminal epithelial cells	Mammary	175
connecting tubule cells	Kidney	169
Gfra3 ID	SMG	137
duct cells	Pancreas	112

E

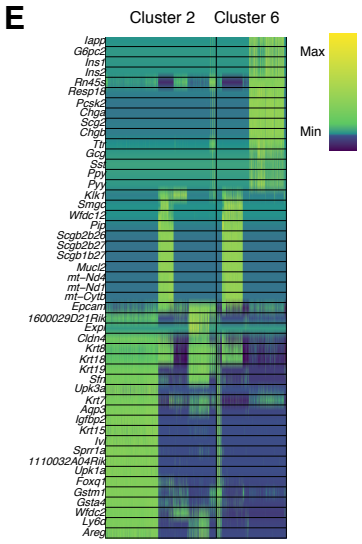

Original annotation from Tabula Muris		Cluster 6 (number of cells)
Gstt1 ID	SMG	391
beta cells	Pancreas	323
alpha cells	Pancreas	250
delta cells	Pancreas	90
T cells	Mammary	75
PP cells	Pancreas	57
Gfra3 ID	SMG	42
LuminalA1	Bladder	38
MesenchymalA1	Bladder	25
MesenchymalB2	Bladder	22

Figure S8. Integration of ID cells with Tabula Muris data.

A) UMAP of unsupervised clustering after integration of ID cells with selected datasets from the Tabula Muris
B) Table showing cluster localization of Gstt1+ and Gfra3+ ID cells. Clusters 2 and 6 contain most ID cells.
C) UMAP of clusters 2 and 6
D) Table showing the 10 most abundant cell types in clusters 2 and 6 based on original annotations from Tabula Muris
E) Heatmap showing expression of the top 25 genes expressed by clusters 2 and 6 compared to all other clusters

TRANSPARENT METHODS

ICR mice

Timed-pregnant ICR females were purchased from Envigo at gestational day E9. From this point onwards mice were cared for and maintained at the NIDCR Veterinary Resource Core in accordance with institutional and IACUC guidelines. All mice were fed ad libitum and kept under 12-hour light/12-hour dark cycle. Pregnant females used for collection of mouse embryos were housed in pairs while those required for collection of P1 pups were individually housed to prevent overcrowding. Mouse embryos were collected from ICR pregnant females at embryonic days E12, E14, and E16, and newborn pups were collected at P1. Additional 30-day old (P30) male and female ICR mice were purchased from Envigo for experimentation.

C3H mice

Adult (10-month old) C3H female mice were obtained from Jay Chiorini's laboratory at NIDCR. Prior to experimentation, these mice were also housed and kept at the NIDCR Veterinary Resource Core in accordance with IACUC guidelines. These mice were used for experimentation upon receipt and were not maintained by our laboratory.

Single-cell Dissociation. SMGs from seven E12 and E14 littermate embryos were separated, isolated and incubated at 37^{o}C for 30 min with 500ul of papain (20U/ml in 1mM L-cysteine with 0.5mM EDTA (Worthington biochemical, New Jersey, USA) in 200ul Eppendorf tubes. Glands were dissociated with a pipette in 5-minute intervals. After 30 min, Papain was inactivated with (1:1) albumin-inhibitor solution (Worthington biochemical, New Jersey, USA) and the cell suspension was collected by centrifugation at 400g at 4^{o}C for 10 min, washed twice and resuspended in Hanks balanced salt solution (HBSS 1x, Gibco, USA) with 1% Bovine serum albumin solution (BSA, Sigma-Aldrich).

SMGs from 2-4 E16 embryos and P1 mice were isolated and enzymatically dissociated in 5ml of digestion cocktail containing Collagenase II (100mg/ml), Hyaluronidase (50mg/ml), deoxyribonuclease (40mg/ml), and neutral protease (50mg/ml) in HBSS-BSA. Dissociation was performed in a 15ml gentleMACS C tube using a miltenyi gentleMACS Octo Dissociator following their preset dissociation program A (24 seconds of clockwise-counterclockwise spin cycles) followed by 30 min incubation at 37^{o}C. Dissociated cells were centrifuged (400xg) for 10 min and resuspended in HBSSA-BSA. Then, cells were passed through 100 μm, 40 μm, and 20 μm filters centrifuging (400xg) for 5 min and resuspending in HBSS-BSA after each filtration step. The final cell suspension was centrifuged (400xg) 5 min and treated with Papain as described above.

For P30 ICR and adult C3H mice, glands were dissociated in a 15ml gentleMACS C tube with 5ml of digestion cocktail prepared with the human tumor dissociation kit (#130-095-929, Miltenyi Biotech, Auburn CA) in RPMI 1640 w/L-Glutamine (Cell applications, Inc, USA). 2 SMGs from male and female ICR mice, and 2 SMG from adult female C3H mice were processed individually. Similar to previous dissociations, digestion was performed in a Miltenyi gentleMACS Octo Dissociator but following the preset 37C_h_TDK_2 program. We added 5ml of RPMI media to the dissociated cells and centrifuged (400xg) for 10 min. Cells were resuspended in RPMI 1640 w/L-Glutamine with 5% PenStrep (Gibco, USA) and washed twice with RPMI. Next, cells were centrifuged (400g) for 5 min and washed with RPMI medium before each filtration step through 70 μm and 40 μm filters. Apart from the enzymatic digestion, all

steps were performed on ice. Single-cell dissociation was confirmed by microscopic examination and cell concentration determined with a Cellometer (Nexcelom Biosciences). Cell concentration was adjusted to $5x10^5$ – $1x10^6$ cells/ml prior to analysis with a 10X genomics Next GEM Chromium controller.

Library prep and sequencing: Single-cell RNA-seq library preparation was performed at the NIDCR Genomics and Computational Biology Core using a Chromium Single Cell v3 method (10X Genomics) following the manufacturer's protocol. Pooled single-cell RNA-seq libraries were sequenced on a NextSeq500 sequencer (Illumina). Cell Ranger Single-Cell Software Suite (10X Genomics) was used for demultiplexing, barcode assignment, and unique molecular identifier (UMI) quantification using the mm10 reference genome (Genome Reference Consortium Mouse Build 38) for read alignment.

Computational analysis: Cell Ranger files were imported to SEURAT v3 using R & R Studio software and processed for clustering following their default pipeline. As a quality control measure, cells with fewer than 200 genes were not included in subsequent analyses, and those with >5% of UMIs mapping to mitochondrial genes were defined as non-viable or apoptotic and were also excluded. A threshold of >10% was used for P30 and adult glands because inherently higher percentage of mitochondrial genes was detected in specific duct populations, and the 5% threshold would therefore filter out these specific cells disproportionately. A similar approach has been recommended for human tissues because a threshold of 5% fails to accurately discriminate between low-quality and healthy cells in ~30% of the evaluated tissues (Osorio and Cai, 2020). Normalization and scaling were performed following SEURAT's default pipeline. All developmental stages were processed individually except for P30 and adult glands, which were integrated prior to assigning cell annotations. The optimal number of PCs for clustering was determined for each individual file using the 'ElbowPlot' function. Cell type labels were assigned based on the expression of known cell type markers summarized in supplementary figure S1. After cell type annotations, data integration with SEURAT was performed for embryonic stages and postnatal stages separately to generate the UMAPs in Figure 1 for visualization only. Data integration of all datasets was used for trajectory inference analysis (Figure 5) with Dynverse (Saelens et al., 2019) and PAGA (Wolf et al., 2019) packages, and for differential expression across developmental stages with SEURAT (Figures 6-7).

Computational separation and analysis of epithelial clusters: Epithelial populations were computationally separated from the previously annotated datasets containing cell type labels using SEURAT's subset function. Epithelial subsets from each stage were re-normalized and scaled to generate new SEURAT objects. Cluster-defining genes were determined using the 'FindAllMarkers' function for unsupervised epithelial clusters.

Trajectory inference analysis: Data integration was performed for all annotated epithelial subsets with SEURAT. This function automatically determined the 2000 most variable genes used as anchors for the analysis. The resulting gene expression matrix and the genes used for integration were then used as input for trajectory analysis with Dynverse. Based on Dynverse guidelines, trajectory inference analysis was performed with the Partition-based graph abstraction (PAGA) algorithm, which determines a pseudotime score and trajectory topology starting from a selected cell population. Because E12 salivary progenitors give rise to the entire salivary epithelium in the adult, E12 epithelial cells were manually selected as the 'root' of the inferred trajectory.

Bhlha15-correlation analysis: End bud, proacinar, and acinar populations were separated from the integrated SEURAT file to extract a gene expression matrix for these populations. Correlation to Bhlha15 gene expression was performed using the 'cor.test' function in R. The resulting correlation scores and p-values are provided in Supplementary File 3 and the top 10 positive and negative correlations were plotted using the 'corrplot' package.

Analysis of developmental transitions: Differential expression between specific populations from the integrated file containing epithelial cells from all stages was performed using the SEURAT 'FindMarkers' function. In order to identify transcription factors, we cross-referenced the resuling differentially expressed genes agains a database of mouse transcription factors (Schmeier *et al*, 2017).Only the top 5 transcription factors (if present) are shown in violin plots using an adjusted p value <0.05 as a measure of significance. The complete list of identified markers is provided in Supplementary File 4.

Immunohistochemistry: Isolated glands were fixed in 4% paraformaldehyde overnight at 4°C. The tissue was dehydrated with gradient ethanol (2 hours for each dehydration step) and placed in 70% Ethanol until the day of standard paraffin embedding. 5μm sections were deparaffinized with xylene substitute for 10 minutes and rehydrated with reverse ethanol gradient for 5 minutes each. Tissue sections were washed twice in each eathanol concentration (90, 70, and 50%) and then placed in distilled water for 10 min. Following rehydration, heat induced antigen retrieval was done in a pressure cooker for 20 min using a pH 9.0 Tris-EDTA homemade prepared with Tris Base (1.21g), ETDA (0.37g) in 100mL of distilled waster. Sections were washed for 5 minutes with homemade 0.1% PBS-Tween (PBST) using 1XPBS (Quality Biologiocal, Gaithersburg, MD) and Tween20 (Quality Biological, Inc). Non-specific binding sites were blocked using the M.O.M.® (Mouse on Mouse) Immunodetection Kit (Vector Laboratories, Burlingame, CA) for 1 hour at room temperature followed by overnight incubation at 4°C with primary antibodies. Tissue sections were washed 3 times for 5 minutes each with PBST and inclubated in secondary antibodies at room temperature for 45 min. Nuclear staining was done with Hoechst (Thermo Fisher Scientific, Marietta, OH) and coverslips were mounted with Fluoro-Gel (Electron Microscopy Sciences, Hatfield, PA). A complete list of antibodies used and their respective dilutions is shown in the Key Resource Table associated with this manuscript.

Wholemount staining: SMGs from E12, E14, and E16 mouse embryos were dissected and fixed with 1:1 Acetone-Methanol at -20°C for 10 minutes. After fixation, glands were washed with 1XPBS and blocked with M.O.M kit for an hour at room temperature. Incubation in primary antibody was performed overnight at 4°C followed by a 1-hour incubation in secondary antibody at room temperature. Glands were mounted on standard microscopy glass slides with Fluoro Gel mounting media. A complete list of antibodies used and their respective dilutions is shown in the Key Resource Table associated with this manuscript.

qRT-PCR: Gene expression of selected markers was measured by qRT-PCR. DNase-free RNA was isolated from whole gland SMG lysates from P20, P30, and P90 male and female ICR mice using the RNAqueous-4PCR kit and DNase removal reagent (Ambion, Inc. Austin, TX). cDNA (20ng) was generated and analyzed by qPCR using SuperScript™ III First-Strand Synthesis System (ThermoFisher Scientific). Melt curve analysis was used to verify the generation of a single amplicon. Expression levels were normalized by the delta-delta Ct method to the housekeeping gene *Rsp29* and aged-matched female glands. Four biological replicates for each group were processed in duplicates except when otherwise specified. Primers were designed using Beacon Designer software and sequences are available in Supplementary File 8.

RNAprobes: Adult p30 and p1, freshly dissected tissue and collected in 200ul eppedorf tubewas and then washed in 1x PBS RNAse free solution. All tools were cleaned with 70% ethanol and wiped before use. All tissue must be preserved in RNAse free solution. Freshly prepared tissue was placed in 4% PFA for no longer 36hrs and sent to ACD with for RNA in situ hybridization with respective probes. Sample were also accompanied by dehydration pockets to remove mosture from prepared slides and slide were immediately placed in 4^{o}C prior to imaging. Specific probe sequences are proprietary and generated with RNAscope® technology by Advanced Cell Diagnostics.

Quantification and statistical analysis

For computational analyses with SEURAT, all statistics were performed using their pipeline's default statistical test, which is based on non-parameteric Wilcoxon rank sum test. Adjusted p-values of <0.05 were chosen as a measure of significance. Correlation analysis was performed using the 'cor.test' function, which uses Pearson's method for significance. For statistical analysis of qRT-PCR data, log-transformed fold changes were compared between male glands and age-mathched female samples using a two-tailed unpaired t-test for each gene individualy.

KEY RESOURCES TABLE

REAGENT or RESOURCE		SOURCE	IDENTIFIER
Antibodies			
AQP5	1:200	Alomone labs	AQP-005
Cytokeratin-5	1:200	Covance	PRB-160P
Cytokeratin-14	1:200	Covance	PRB-155P
GFR alpha-3/GDNF R alpha-3	1:80	R&D systems	AF2645
GSTT1	1:200	Lifespan Bioscience	LS-B10781
Epcam	1:200	Abcam	Ab71916
NKCC1	1:200	Santa Cruz Biotechnology	sc-21547
Vimetin	1:200	Abcam	Ab8978
Smgc	1:100	Lifespan Bioscience	LS-C154825
Mist1	1:200	Cell signaling	14896
Mist1	1:100	Santa Cruz Biotechnology	sc-80984
PSP/Bpifa2	1:100	Lifespan Bioscience	LS-B9833
Lpo	1:100	Thermo Fischer Scientific	PA1-46353
Claudin10	1:200	Thermo Fischer Scientific	38-8400
Alexa Fluor® 488 AffiniPure $F(ab')_2$ Fragment Donkey Anti-Goat IgG (H+L)	1:250	Jackson Immunoresearch Laboratories	705-546-147
Alexa Fluor® 647 AffiniPure $F(ab')_2$ Fragment Donkey Anti-Goat IgG (H+L)	1:250	Jackson Immunoresearch Laboratories	705-606-147
Alexa Fluor® 488 AffiniPure $F(ab')_2$ Fragment Donkey Anti-Rabbit IgG (H+L)	1:250	Jackson Immunoresearch Laboratories	711-546-152
Cy™3 AffiniPure $F(ab')_2$ Fragment Donkey Anti-Rabbit IgG (H+L)	1:250	Jackson Immunoresearch Laboratories	711-166-152
Cy™3 AffiniPure $F(ab')_2$ Fragment Donkey Anti-Mouse IgG (H+L)	1:250	Jackson Immunoresearch Laboratories	715-165-150
Hoechst 33342	1:1000	Thermo Fisher Scientific	H3570
Oligonucleotides – Sequences provided in Supplementary File 8			
Smgc		Life Technologies	N/A
Dcdc2a		Life Technologies	N/A
Serpinb11		Life Technologies	N/A
Gstt1		Life Technologies	N/A
Kit		Life Technologies	N/A
Gfra3		Life Technologies	N/A
Esp18		Life Technologies	N/A
Nkd2		Life Technologies	N/A
Rs29		Life Technologies	N/A
RNA probe for Aqp5		ACDBio	N/A
RNA probe for Esp18		ACDBio	N/A
RNA probe for Gfra3		ACDBio	N/A
RNA probe for Nkd2		ACDBio	N/A
RNA probe for Prol1		ACDBio	N/A
RNA probe for Ret		ACDBio	N/A

Chemicals, Peptides, and Recombinant Proteins		
Hanks balanced salt solution (HBSS) no calcium, no magnesium, no phenol red	Gibco/ Life technologies	14175-103
PBS 1X	Quality Biological, Inc	114-058-101
Tween 20	Quality Biological, Inc	A611-M147-13
Fluoro-Gel with TRIS mounting media	Electron Microscopy Sciences	1798510
Bovine serum albumin solution (BSA)	Sigma Aldrich	A9205
16% Paraformaldehyde (formaldehyde) Aqueous solution	Electron Microscopy Sciences	15700
Xylene substitute	Sigma Aldrich	A5597-1GAL
Ethanol 100%	Sigma Aldrich	E7023
Ethanol 95%	Sigma Aldrich	493538
Acetone	Sigma Aldrich	179973
Methanol	ThermoFisher	A412-4
Tris Base	Millipore Sigma	648310-M
EDTA	Millipore Sigma	E1161
RPMI 1640	Cell application	185-500
Neutral Protease	Worthington Biochemical Corp	LS02109
Deoxyribonuclease I	Worthington Biochemical Corp	LS002145
Hyaluronidase	Worthington Biochemical Corp	LS002594
Collagenase, Type 2	Worthington Biochemical Corp	LS00476
Critical Commercial Assays		
Human tumor dissociation kit	Miltenyi Biotech	130-095-929
M.O.M (Mouse on Mouse) Immunodetection Kit	Vector Laboratories	BMK-2202,
Superscript III First-Strand Synthesis System	Life Technologies	18080051
Papain Dissociation system	Worthington Biochemical	LK003150
Deposited Data		
scRNAseq of murine SMG at multiple developmental stages	This paper	GSE15032
Experimental Models: Organisms/Strains		
Timed-pregnant ICR Female Mice	Envigo	ICR (CD-1®)
ICR postnatal mice	Envigo	ICR (CD-1®)
C3H adult female mice	From Jay Chiorini's lab	N/A
Software and Algorithms		
R & R studio	https://rstudio.com/	N/A
Cell Ranger	10X Genomics	N/A
SEURAT	Stuart, Butler *et al* (2019)	N/A
Dynverse	Saelens *et al* (2019)	N/A
PAGA	Wolf A *et al* (2019)	N/A
Other		
MACS SMART Strainers 70μm	Miltenyi Biotech	130-110-916

Supplementary references

Arany, s., catalan, m. A., roztocil, e. & ovitt, c. E. 2011. Ascl3 knockout and cell ablation models reveal complexity of salivary gland maintenance and regeneration. *Dev biol,* 353**,** 186-93.

Dohan, o., de la vieja, a., paroder, v., riedel, c., artani, m., reed, m., ginter, c. S. & carrasco, n. 2003. The sodium/iodide symporter (nis): characterization, regulation, and medical significance. *Endocr rev,* 24**,** 48-77.

Hazen-martin, d. J., landreth, g. & simson, j. A. 1987. Immunocytochemical localization of nerve growth factor in mouse salivary glands. *Histochem j,* 19**,** 210-6.

Johnson, c. L., kowalik, a. S., rajakumar, n. & pin, c. L. 2004. Mist1 is necessary for the establishment of granule organization in serous exocrine cells of the gastrointestinal tract. *Mech dev,* 121**,** 261-72.

Larsen, h. S., aure, m. H., peters, s. B., larsen, m., messelt, e. B. & kanli galtung, h. 2011. Localization of aqp5 during development of the mouse submandibular salivary gland. *J mol histol,* 42**,** 71-81.

Schmeier S., Alam, T., Essack M., and Bajic V., 2017. TcoF-DB v2: update of the database of human and mouse transcription co-factors and transcription factor interactions. *Nuc Ac Res*, 45, D145-150.

Zeng, m., szymczak, m., ahuja, m., zheng, c., yin, h., swaim, w., chiorini, j. A., bridges, r. J. & muallem, s. 2017. Restoration of cftr activity in ducts rescues acinar cell function and reduces inflammation in pancreatic and salivary glands of mice. *Gastroenterology,* 153**,** 1148-1159.